

576. Simulation of oscillation dynamics of mechanical system with the electrorheological shock-absorber

V. Bilyk¹, E. Korobko², A. Binshtok³, A. Bubulis⁴

^{1,2} Luikov A.V. Heat and Mass Transfer Institute of NAS of Belarus,

P. Brovki str. 15, 220072, Minsk, Belarus

e-mail: *snowsoft@tut.by*¹; *eva@itmo.by*²

³ Minsk Wheel Tractor Plant (MWTP),

Partizansky ave. 105, 220021, Minsk, Belarus

e-mail: *albinshtok@gmail.com*

⁴ Kaunas University of Technology,

Kęstučio 27, LT-44312, Kaunas, Lithuania

e-mail: *algimantas.bubulis@ktu.lt*

(Received 25 September 2010; accepted 9 December 2010)

Abstract. The paper presents the development of mathematical model of oscillating system by taking into account electrorheological (ER) characteristics. Characteristics of the ER shock-absorber (dependences of force on value of control electric signal considering shock-absorber geometry, rod displacement, rheological properties of ER fluid) are calculated. Comparison of simulation results of shock-absorber characteristics with experimental findings is performed. Analysis of calculated relations of amplitudes of output and input signals depending on value of a control electric signal is carried out.

Keywords: oscillation system, three degrees of freedom, electrorheological shock-absorber, numerical integration, rheological properties, electrorheological fluid, yield stress, viscosity.

Introduction

There is a constant stiffening of technical requirements imposed on vibro-protection of structural elements of a vehicle and driver in the European countries and the rest of the world. Currently active and semi-active cushioning systems are even more frequently applied to the solution of this problem. Such controlled systems are increasingly needed in the modern motor car and tractor construction industry.

One of the key questions of development of adaptive cushioning systems is engineering design of devices with controlled elastic or damping characteristics. The most simple and technological of such devices are shock-absorbers using smart materials (electro- and magneto-rheological fluids) with properties, which change upon external influences, in particular, electric or magnetic fields.

Mathematical model of a damper, allowing to present its performance data by the instrumentality of approximating dependences, is proposed in [1]. Mathematical models of controlled shock-absorbers, considering features of rheological properties of working electrosensitive damping fluid, are described in [2-6]. Commonly rheological properties of electrorheological (ER) fluid are described by visco-plastic model of Shvedov-Bingham [5-9]. As practice shows, such simplified model is convenient for technical calculations of shock-absorber performance characteristic.

The most important task in engineering process of adaptive systems is prediction of overall performance of shock-absorber in oscillatory system. Experimental or theoretical research techniques are used for this purpose [4-11]. Modeling of shock-absorber performance characteristics in oscillatory system is the fastest and the most economical way for estimating its operating modes. Therefore construction of mathematical model of oscillatory system with the designed shock-absorber is the most effective way to adjust its characteristics to the technical requirements [12, 13].

The purpose of this work is numerical modeling and the analysis of oscillation dynamics of mechanical system of a quarter of vehicle suspension with the designed ER shock-absorber during forced oscillations and while it is moving through “sleeping policeman”. Characteristics of the ER shock-absorber with non-Newtonian ER fluid have been experimentally investigated by the authors earlier [14].

1. Statement of a mathematical problem

Let's consider block diagrams with passive (Fig. 1) and active (Fig. 2) 3-mass oscillation systems which represent the mechanics of a quarter of vehicle suspension.

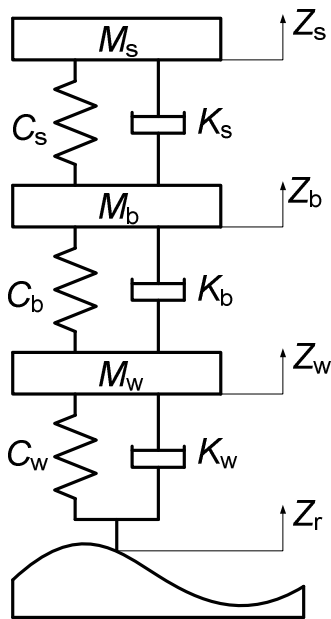


Fig. 1. The scheme of 3-mass oscillation system with passive viscous-elastic elements

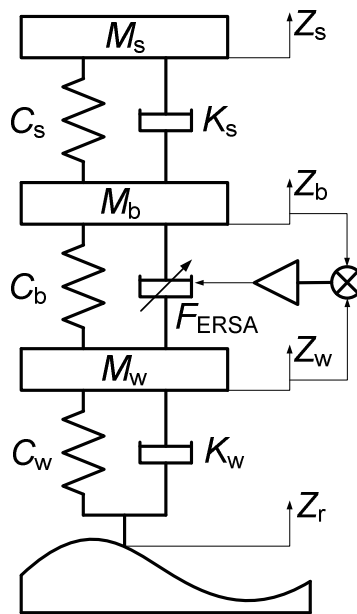


Fig.2. The scheme of 3-mass oscillation system with controlled ER shock-absorber

The difference between these models is use of the controlled shock-absorber with ER fluid in the active system (Fig. 2) instead of the shock-absorber with constant damping coefficient K_b in the passive one (Fig. 1).

The passive oscillatory system (Fig. 1) can be described by the system of the differential equations:

$$M_s \ddot{z}_s + K_s (\dot{z}_s - \dot{z}_b) + C_s (z_s - z_b) = 0, \quad (1)$$

$$M_b \ddot{z}_b - K_s (\dot{z}_s - \dot{z}_b) - C_s (z_s - z_b) + K_b (\dot{z}_b - \dot{z}_w) + C_s (z_b - z_w) = 0, \quad (2)$$

$$M_w \ddot{z}_w - K_b (\dot{z}_b - \dot{z}_w) - C_b (z_b - z_w) + K_w (\dot{z}_w - \dot{z}_r) + C_w (z_w - z_r) = 0, \quad (3)$$

where M , K and C are the mass, coefficients of damping and stiffness; z , $\dot{z}_s = \partial z_s / \partial t$ and $\ddot{z}_s = \partial^2 z_s / \partial t^2$ is the displacement, velocity and acceleration respectively; t is the time variable; indexes r , s , b , w , r are the road, seat, body and wheel respectively.

A working fluid with non-Newtonian properties is used in the ER shock-absorber. Effective viscosity of fluid and damping force of the shock-absorber accordingly are changed at influence of an controlled electric signal, therefore the system of the equations (1)-(3) for active oscillatory system (Fig. 2) is as follows:

$$M_s \ddot{z}_s + K_s (\dot{z}_s - \dot{z}_b) + C_s (z_s - z_b) = 0, \quad (4)$$

$$M_b \ddot{z}_b - K_s (\dot{z}_s - \dot{z}_b) - C_s (z_s - z_b) + F_{ERSA} + C_s (z_b - z_w) = 0, \quad (5)$$

$$M_w \ddot{z}_w - F_{ERSA} - C_b (z_b - z_w) + K_w (\dot{z}_w - \dot{z}_r) + C_w (z_w - z_r) = 0, \quad (6)$$

where F_{ERSA} – force of the electrorheological shock-absorber.

The mathematical model of the ER shock-absorber, which enables determination of its damping force F_{ERSA} , should take into consideration shock-absorber geometry, rheological properties of a working fluid (its visco-plastic parameters), rod motion and value of controlled signal (intensity of electric field).

1.1 Mathematical model of the ER shock-absorber

We use the cylindrical coordinate system for the ER shock-absorber geometry (Fig. 3).

The following assumptions are used: 1) flow regime in annular gap of the ER shock-absorber is completely developed; 2) laminar flow; 3) the electrorheological fluid is incompressible; 4) the annular gap has sufficient length, therefore the end effects may be neglected; 5) at the channel walls the ERF velocity is equal to zero (sticking condition).

Then the motion equation of a fluid in the shock-absorber channel is:

$$\frac{1}{r} \frac{d}{dr} (r\tau) = -\frac{\Delta P}{L}, \quad (7)$$

where ΔP – pressure drop in an annular gap of shock-absorber, Pa; r – radius, m.

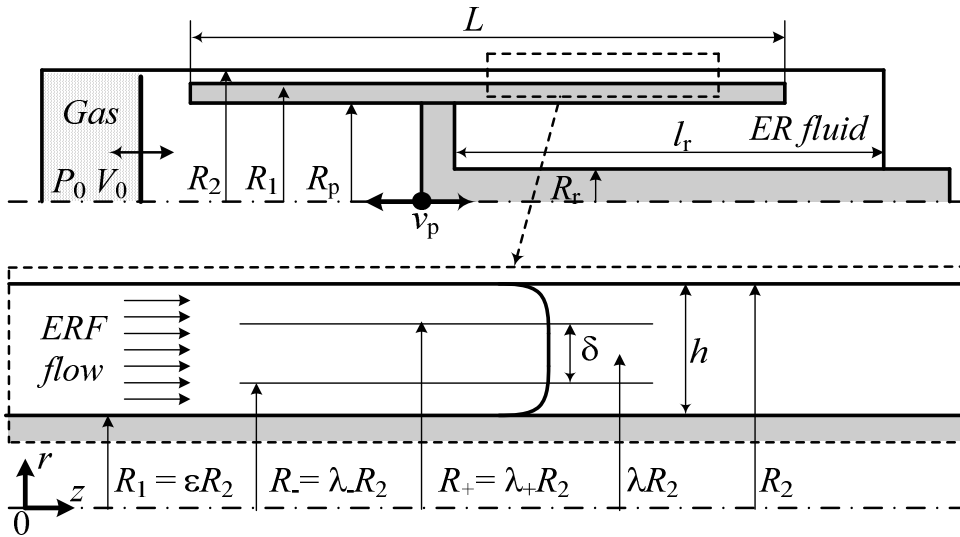


Fig. 3. The scheme of ERF flow in the annular gap of the ER shock-absorber in cylindrical system coordinates. R_1, R_2, R_p, R_r – radii of the internal and the external wall of annular channel, piston and rod accordingly; $\varepsilon, \lambda, \lambda_-, \lambda_+$ – dimensionless parameters of radii; δ – dimensionless width of quasi-solid kernel of ERF flow in the annular channel; r, z – axes and variables in cylindrical system coordinates; «-» и «+» – indexes of the bottom and top borders quasi-solid kernel; V_0 and P_0 – volume and pressure in the pneumatic chamber at completely extended rod from the shock-absorber; h and L – a thickness and length of the annular channel; l_r – depth of immersing of a rod in a shock-absorber chamber.

At radius $r = \lambda R_2$ (where λ is the integration constant and represents the dimensionless parameter at which shear stress is equal to zero [15]) the motion equation and rheological Shvedov-Bingham equation are:

$$\tau = -\frac{\Delta P R_2}{2L} \left(\frac{r}{R_2} - \frac{\lambda^2 R_2}{r} \right) \quad (8)$$

$$\tau = \pm \tau_0 - \mu_p \frac{du}{dr} = \pm \tau_0 - \mu_p \dot{\gamma} \quad (9)$$

where the sign «+» – momentum transfer in direction +r and «-» for direction -r; τ_0 – yield stress, Pa; μ_p – plastic viscosity, Pa·s; $\dot{\gamma} = du/dr$ – shear rate, c^{-1} .

The effective viscosity μ_e is defined as

$$\mu_e = \frac{\tau}{\dot{\gamma}} = \left| \frac{\tau_0}{\dot{\gamma}} \right| + \mu_p \quad (10)$$

Let's enter the dimensionless variables of shear stress τ^* , yield stress β_0 , rate φ , radial coordinate ρ and relations of radiuses of annular gap ε :

$$\tau^* = \frac{2\tau L}{R_2 \Delta P}; \quad (11)$$

$$\beta_0 = \frac{2\tau_0 L}{R_2 \Delta P}; \quad (12)$$

$$\varphi = \frac{2\mu_p L}{R_2^2 \Delta P} u; \quad (13)$$

$$\rho = \frac{r}{R_2}; \quad (14)$$

$$\varepsilon = R_1/R_2. \quad (15)$$

Then the equations (8)–(9) are

$$\tau^* = \rho - \frac{\lambda^2}{\rho}; \quad (16)$$

$$\tau^* = \pm\beta_0 - \mu_p \frac{d\varphi}{d\rho}. \quad (17)$$

Integrating the equations (16)–(17) on a variable ρ with conditions $\varphi(\rho = \varepsilon) = 0$ and $\varphi(\rho = 1) = 0$ and considering three areas of ERF flow in the annular channel (Fig. 3), we obtain

$$\varphi_- = -\beta_0(\rho - \varepsilon) - \frac{1}{2}(\rho^2 - \varepsilon^2) + \lambda^2 \ln \frac{\rho}{\varepsilon}, \text{ at } \varepsilon \leq \rho \leq \lambda_-; \quad (18)$$

$$\varphi_0 = \varphi_-(\lambda_-) = \varphi_+(\lambda_+), \text{ at } \lambda_- \leq \rho \leq \lambda_+; \quad (19)$$

$$\varphi_+ = -\beta_0(1 - \rho) + \frac{1}{2}(1 - \rho^2) + \lambda^2 \ln \rho, \text{ at } \lambda_+ \leq \rho \leq 1. \quad (20)$$

Using the auxiliary equations $\lambda^2 = \lambda_+(\lambda_+ - \beta_0)$ and $\lambda_- = \lambda_+ - \beta_0$, condition of equality $\varphi_-(\lambda_-) = \varphi_+(\lambda_+)$ we can write as

$$2\lambda_+(\lambda_+ - \beta_0) \ln \frac{\lambda_+ - \beta_0}{\varepsilon \lambda_+} - 1 + (\beta_0 + \varepsilon)^2 + 2\beta_0(1 - \lambda_+) = 0. \quad (21)$$

Expression for definition of volume flow rate Q , is solved by integration of the equations (18)–(20) on the annular gap and after a number of transformations it acquires the following form:

$$Q = \frac{\pi R_2^4 \Delta P}{8\mu_p L} \left[(1 - \varepsilon^4) - 2\lambda_+(\lambda_+ - \beta_0)(1 - \varepsilon^2) - \frac{4\beta_0}{3}(1 + \varepsilon^3) + \frac{\beta_0}{3}(2\lambda_+ - \beta_0)^3 \right]. \quad (22)$$

Transforming the expression (22), where the volume flow rate of ER fluid $Q = v_p \pi (R_p^2 - R_r^2)$ at piston velocity of the ER shock-absorber v_p , and having parameters of a yield stress, dynamic viscosity and the annular gap geometry, it is possible to find the values β_0 and λ_+ from the equation system:

$$2\lambda_+(\lambda_+ - \beta_0) \ln \frac{\lambda_+ - \beta_0}{\varepsilon\lambda_+} - 1 + (\beta_0 + \varepsilon)^2 + 2\beta_0(1 - \lambda_+) = 0; \quad (23)$$

$$\frac{\pi R_2^3 \tau_0}{4\mu_e \beta_0} \left[(1 - \varepsilon^4) - 2\lambda_+(\lambda_+ - \beta_0)(1 - \varepsilon^2) - \frac{4\beta_0}{3}(1 + \varepsilon^3) + \frac{\beta_0}{3}(2\lambda_+ - \beta_0)^3 \right] = v_p \pi (R_p^2 - R_r^2). \quad (24)$$

We solve system of the equations (26) - (27) with variables β_0 and λ_+ . Having found numerical value of parameter β_0 , we define pressure difference ΔP in the annular channel according to (12).

Now it is possible to calculate shock-absorber performance characteristics, for example, shock-absorber depending on displacement or velocity of rod motion.

Created damping force of telescopic one-ring pneumatic hydraulic shock-absorber F_{ERSA} can be defined as:

$$F_{ERSA} = F_f + F_g + F_{ERF}, \quad (25)$$

where F_f , F_g , F_{ERF} – forces of dry friction, gas resistance and hydraulic resistance of ER fluid.

Force of inertia of the shock-absorber piston is very small in comparison with damping force of the shock-absorber, therefore we neglect it.

Each force is described by the following expression:

$$F_f = (F_0 + c_1 \Delta P) \operatorname{sgn}(v_p); \quad (26)$$

$$F_g = P_0 \left[\frac{V_0}{V_0 - A_r(l_r - z)} \right]^n A_r; \quad (27)$$

$$F_{ERF} = (A_p - A_r) \Delta P. \quad (28)$$

where A_p , A_r – the cross-section area of piston and rod accordingly; F_0 and c_1 – the parameters defining dry friction force from experiment; n - exponent of power.

It is necessary to know rheological properties of ER fluid (parameters of dynamic viscosity and yield stress) for calculation of pressure drop in the annular channel and shock-absorber force according to expression (9).

1.2 Rheological properties of ER fluid

Two-component ER fluid “ERF-3” has been developed in laboratory conditions [16]. Measurements of rheological properties of the ER fluid are executed in a range of shear rates 1-3500 c^{-1} on rheometer “Physica MCR 301” of manufacturer «Anton Haake» with a high-voltage measuring cell which represents system of coaxial cylinders. Rheological curves are constructed for various values of electric field strength by results of experimental investigation. All of them can be described by visco-plastic model of Shvedov-Bingham:

$$\tau = \tau_{yd} + \mu_d \dot{\gamma}, \quad (29)$$

where τ_{yd} – dynamic yield stress, Pa; μ_d – dynamic viscosity, Pa·s.

Rheological model (29) is used in mathematical model of the ER shock-absorber (9).

It is noticed, that dynamic viscosity for given formulation ERF-3 at investigated shear rate weakly depends on electric field strength, but depends on temperature in observable range 20-

80°C [16]. Dependence of dynamic viscosity with respect to various values of temperature without dependence on electric field strength is defined as:

$$\mu_d = \mu_0 \cdot \exp(E_a / R / (T + 273.15)), \quad (30)$$

where $\mu_0 = 0.000122 \text{ Pa}\cdot\text{s}$ – dynamic viscosity at temperature $T = 0^\circ\text{C}$; E_a – energy of activation (16436.3 J); R – universal gas constant; T – fluid temperature, °C.

According to experimental investigations of yield stress [16] dependence of static yield stress τ_{ys} vs. electric field strength is defined as:

$$\tau_{ys} = c_s \cdot E + \tau_{0s} \quad (31)$$

where τ_{0s} – static yield stress at value of electric field strength $E = 0 \text{ kV/mm}$; E – electric field strength, kV/mm; c_s – parameter, which indicates growth intensity of static yield stress on value of electric field strength.

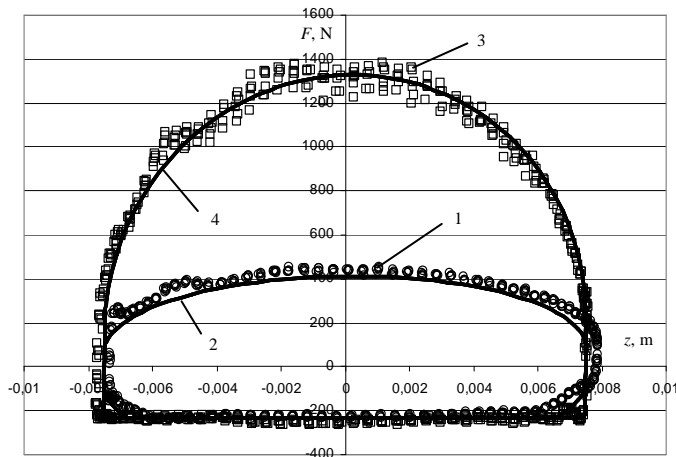
As it is proposed in work [9], yield stress τ_0 in the equation (9) uses static yield stress τ_{ys} .

2. Numerical modeling of oscillation dynamics of mechanical system, performance characteristics of the ER shock-absorber and comparison with experiment

For calculation of characteristics of the ER shock-absorber we use the following data: $R_r = 0.008 \text{ m}$; $R_p = 0.02 \text{ m}$; $R_1 = 0.023 \text{ m}$; $R_2 = 0.024 \text{ m}$; $h = (R_2 - R_1)/2 = 0.001 \text{ m}$; $L = 0.1 \text{ m}$; $P_0 = 10.5 \text{ MPa}$; $V_0 = 0.000049 \text{ m}^3$; $l_r = 0.04 \text{ m}$; and auxiliary formulas $A_p = \pi R_p^2$; $A_r = \pi R_r^2$.

For calculation of oscillation system we use the following parameters: $K_w = 400 \text{ N}\cdot\text{s/m}$; $C_w = 225000 \text{ N/m}$; $M_w = 31 \text{ kg}$; $K_b = 1500 \text{ N}\cdot\text{s/m}$; $C_b = 29000 \text{ N/m}$; $M_b = 290 \text{ kg}$; $K_s = 3000 \text{ N}\cdot\text{s/m}$; $C_s = 8000 \text{ N/m}$; $M_s = 90 \text{ kg}$.

Experimental data and results of numerical modeling of ER shock-absorber force are provided in Fig. 4 at rod motion under the harmonic law with amplitude of 7.5 mm and frequency of 2 Hz.



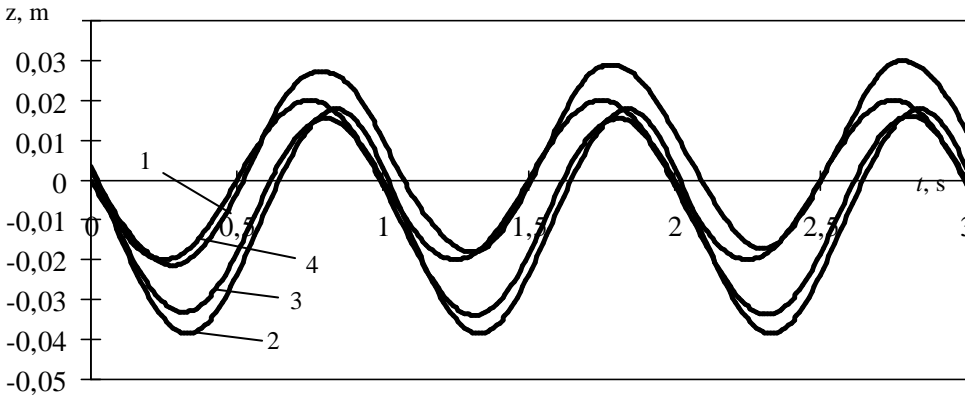
1, 2 – $E = 0 \text{ kV/mm}$; 3, 4 – $E = 2,5 \text{ kV/mm}$.

Fig. 4. The dependence of force of the ER shock-absorber as a function of rod displacement at various values of electrical field strength: experimental values – points (1, 3) and theoretical values – lines (2, 4). Amplitude of rod displacement – 7,5 mm. Frequency of oscillations – 2 Hz.

Comparison of results of experiment and modeling of operating regime of the ER shock-absorber has been performed for amplitudes of rod displacement in the range of 5-25 mm and frequencies in the range of 0,5-5 Hz, and demonstrated good coincidence.

The correctness of numerical calculation of mathematical model of oscillatory system (4)–(6) is confirmed by close fit of task solving results (displacements of sprung weights) test model of passive oscillatory system (1)–(3) and models [17] with its parameters (weight, coefficient of damping and rigidity).

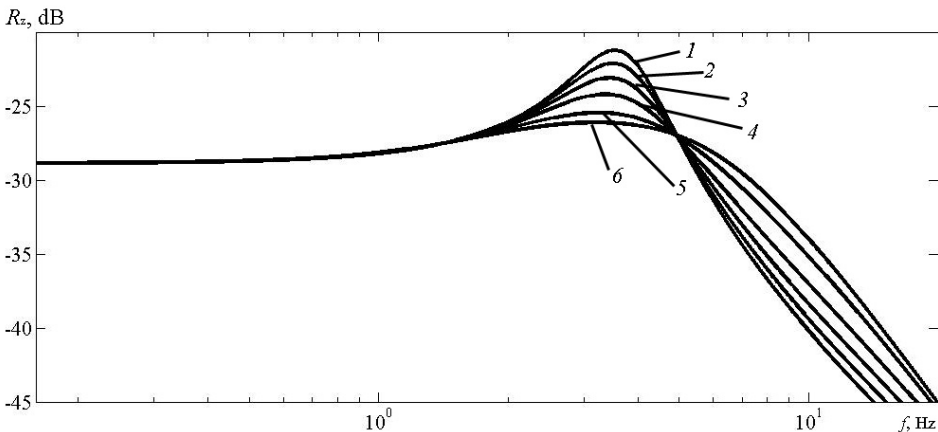
The results of modeling of oscillation dynamics of mechanical system with the ER shock-absorber at the forced oscillation according to system of the differential equations (4)–(6) at various values of electric field strength are illustrated in Fig. 5.



1 – input signal (a road profile z_r); 2 – $E = 0$ kV/mm; 3 – 1,5; 4 – 2,5.

Fig. 5. The dependence of driver seat displacement z_s on time at the forced oscillation with amplitude of 0,02 m and frequency of 1 Hz and at various values of electric field strength

For the work analysis of oscillation system at various frequencies of input signal we can plot the peak-frequency characteristic representing logarithmic dependence of relations of amplitudes of input and output signals $R_z = 20 \text{ Log } (z_s/z_r)$ at various values of the controlled signal (Fig. 6).

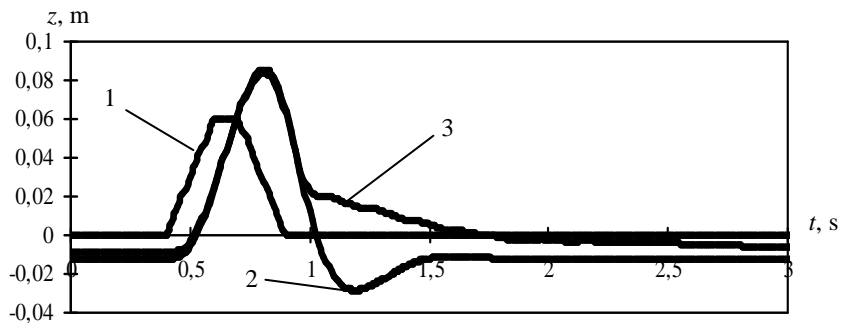


1 – $E = 2,5$ kV/mm; 2 – 2,0; 3 – 1,5; 4 – 1,0; 5 – 0,5; 6 – 0,0.

Fig. 6. The peak-frequency characteristic at various values of controlled signal

Results in Fig. 6 indicate that control efficiency of oscillatory system is ensured in the field of frequencies exceeding 1 Hz. This phenomenon is explained by inertia of oscillation system at small oscillation frequencies when elastic elements (springs) define an operating mode of this system in more degrees, than damping elements (shock-absorbers). At frequency more than 5 Hz the damping of oscillation system is amplified with increase of electric field strength.

Now we investigate active oscillatory system operation during its linear movement with velocity of 30 km/h through “the sleeping policeman” of trapezium-shape according to the standard [18] in the absence of an operating signal and at use of control algorithm [19] (Fig. 7), which works by a principle of make-and-break of control signal depending on a combination of modes of shock-absorber rod stripping (compression and stretching) and movement velocity of cushion weights.



1 – road profile “the sleeping policeman” in time scale; 2 – $E = 0$ kv/mm; 3 – control algorithm [19].

Fig. 7. The temporal variation of driver seat displacement (cushion weight M_s)

As simulation results indicate, time of oscillation damping (from time moment of maximum deviations of a driver seat till the moment of time of absence of periodic oscillations) is equal to 1 s at $E = 0$ kV/mm and less than 0,5 s at motion of the system through an obstacle “the sleeping policeman” by using control algorithm [19]. Thus, efficiency of oscillation damping in time makes more than 2 times at comparison of passive and active oscillation system.

Conclusions

The reported research work proposed a mathematical model of oscillation system taking into account ER shock-absorber characteristics and rheological properties of a working ER fluid. Efficiency of oscillation damping in time is twice as large when comparing passive and active oscillation systems. Analysis of the relation of amplitudes of input and output signals depending on forced oscillation frequency at various magnitudes of electric field strength has revealed that at forced oscillation frequency less than 1 Hz the oscillation system operates essentially in the same manner at various values of control signal. It is demonstrated that at forced oscillation frequency of more than 1 Hz with increase of electric field strength the efficiency of oscillation damping grows (natural frequencies of the investigated oscillation system is equal to 1.4, 2.7 and 8.5 Hz). Performance characteristics of the ER shock-absorber (dependence of force on value of control electric signal taking into account shock-absorber geometry, rod displacement, rheological properties of ER fluid) were calculated. Theoretical and experimental results of the shock-absorber characteristics are in good agreement (relative factor of a variation makes 9-28 % depending on operating mode of the ER shock-absorber).

Acknowledgement

This research was funded by a grant TPA-32/2010 from the Research Council of Lithuania. Work is executed at financial support of the Byelorussian fund of fundamental research (grant 09-136M).

References

- [1] **Stanway R., Sproston J., Firoozian R.** Identification of the Damping Law of an Electro-Rheological Fluid: A sequential Filtering Approach. Transactions of the ASME: Journal of Dynamic Systems Measurement and Control V.111. 1989. P. 91-96
- [2] **Butz T., Stryk O.** Modelling and Simulation of ER and MR Fluid Dampers. Z. angew. Math. Mech. V.82. No.1. 2002. P. 3-20.
- [3] **Suh M. S., Yeo M.S.** Development of Semi-Active Suspension Systems Using ER Fluids for the Wheeled Vehicle. Journal of Intelligent Material Systems and Structures V.10. 1999. P. 743-747.
- [4] **Choi S. B., Han Y. M., Song H. J., Sohn J. W. and Choi H. J.** Field Test on Vibration Control of Vehicle Suspension System Featuring ER Shock Absorbers. Journal of Intelligent Material Systems and Structures V18. 2007. P. 1169-1174.
- [5] **Choi S. B., Choi J. H., Lee Y. S., Han M. S.** Vibration Control of an ER Seat Suspension for a Commercial Vehicle. Journal of Dynamic Systems, Measurement, and Control. V.125. 2003. P. 60-68.
- [6] **Dixon J.C.** The Shock Absorber Handbook: Second Edition. John Wiley & Sons, Ltd, 2007.
- [7] **Wereley N. M.** Nondimensional Herschel_Bulkley Analysis of Magnetorheological and Electrorheological Dampers. Journal of Intelligent Material Systems and Structures. 19. 2008. P. 257-268.
- [8] **Seo M.S., Lee H.G., Kim M.C.** A study on the performance estimation of semi-active suspension system considering the response time of electro-rheological fluid. Electrorheological fluids and magnetorheological suspensions. Nice University, 2001, World Sc.Publishing Co.Pte.Ltd, P. 181-186.
- [9] **Weiss K. D., Coulter J. P., Carlson J. D.** Electrorheological materials and their usage in intelligent material systems and structures, Part I: Mechanisms, Formulations and Properties. ER Materials and Their Usage in Intelligent Material Systems and Structures. Proceedings of the Recent Advances in Adaptive and Sensory Materials and their Applications, C.A. Rogers and Lancaster, Technomic Publishing Company, Inc., 1992. P. 605-621.
- [10] **Vitrani M. A., Nikitzuk J., Morel G., Mavroidis C., Weinberg B.** Torque Control of Electrorheological Fluidic Resistive Actuators for Haptic Vehicular Instrument Controls. Journal of Dynamic Systems, Measurement, and Control. Transactions of the ASME. V.128. 2006. P. 216-226.
- [11] **Wang X., Gordaninejad F.** Dynamic Modeling of Semi-Active ER/MR Fluid Dampers. Damping and Isolation, Proceedings of SPIE Conference on Smart Materials and Structures, V. 4331. Ed. Daniel J. Inman, 2001. P. 82-91.
- [12] **Rotenberg, R. V.** Car suspension. Moscow: Mashinostroenie, 1972.
- [13] **Derbaremdiker A. D.** Vehicle shock-absorbers. Moscow: Mashinostroenie, 1985.
- [14] **Bilyk V. A.** Temperature factor in work of the ER shock-absorber. VI Minsk International Heat and Mass Transfer Forum MIF 2008. 4 pages in electronic pdf-version on site www.itmo.by, HMTI of NAS of Belarus.
- [15] **Smolskii B. M., Shulman Z. P., Gorislavets V. M.** Rheodynamics and Heat Transfer of Nonlinear Viscoplastic Materials. Minsk: Science and Technics. 1970.
- [16] **Korobko E., Novikova Z., Bedzik N., Zhurauski M., Bubulis A., Dragašius E.** Adaptive Fluids for Electrorheological Dampers and their Damping Characteristics. Proceedings of the 8th International Conference "Vibroengineering 2009". Kaunas, Technologija, 2009. P. 27-30.
- [17] **Kiran A.** Analysis of Passive Suspension System using Matlab, Simulink and SimScape. Article in 8 pages on <http://www.mathworks.com/matlabcentral/fileexchange/18410-analysis-of-suspension-system-using-matlab-simulink-and-simscape>, February 10, 2010.
- [18] **STB 1538-2005 BY (Belarus).** Humps on roads and streets: Specification and application procedure.
- [19] **Zhang H, Winner H., Li W.** Comparison between Skyhook and Minimax control strategies for Semi-active Suspension System. World academy of science, engineering and technology. 55. 2009. P. 624-627.